

This article was downloaded by: [Renmin University of China]

On: 13 October 2013, At: 11:07

Publisher: Taylor & Francis

Informa Ltd Registered in England and Wales Registered Number: 1072954 Registered office: Mortimer House, 37-41 Mortimer Street, London W1T 3JH, UK



Molecular Crystals and Liquid Crystals

Publication details, including instructions for authors and subscription information:

<http://www.tandfonline.com/loi/gmcl20>

Improved Signal-to-Noise Ratio of Green-Sensitive Organic Photoconductive Device by Doping Silole Derivative

Takeshi Fukuda^a, Sho Kimura^a, Norihiko Kamata^a, Keita Mori^a & Ken Hatano^a

^a Department of Functional Materials Science, Saitama University, 255 Shimo-Okubo, Sakura-ku, Saitama, Japan

Published online: 02 Sep 2013.

To cite this article: Takeshi Fukuda, Sho Kimura, Norihiko Kamata, Keita Mori & Ken Hatano (2013) Improved Signal-to-Noise Ratio of Green-Sensitive Organic Photoconductive Device by Doping Silole Derivative, *Molecular Crystals and Liquid Crystals*, 578:1, 119-126, DOI: [10.1080/15421406.2013.804784](https://doi.org/10.1080/15421406.2013.804784)

To link to this article: <http://dx.doi.org/10.1080/15421406.2013.804784>

PLEASE SCROLL DOWN FOR ARTICLE

Taylor & Francis makes every effort to ensure the accuracy of all the information (the "Content") contained in the publications on our platform. However, Taylor & Francis, our agents, and our licensors make no representations or warranties whatsoever as to the accuracy, completeness, or suitability for any purpose of the Content. Any opinions and views expressed in this publication are the opinions and views of the authors, and are not the views of or endorsed by Taylor & Francis. The accuracy of the Content should not be relied upon and should be independently verified with primary sources of information. Taylor and Francis shall not be liable for any losses, actions, claims, proceedings, demands, costs, expenses, damages, and other liabilities whatsoever or howsoever caused arising directly or indirectly in connection with, in relation to or arising out of the use of the Content.

This article may be used for research, teaching, and private study purposes. Any substantial or systematic reproduction, redistribution, reselling, loan, sub-licensing, systematic supply, or distribution in any form to anyone is expressly forbidden. Terms & Conditions of access and use can be found at <http://www.tandfonline.com/page/terms-and-conditions>

Improved Signal-to-Noise Ratio of Green-Sensitive Organic Photoconductive Device by Doping Silole Derivative

TAKESHI FUKUDA,* SHO KIMURA, NORIHIKO KAMATA,
KEITA MORI, AND KEN HATANO

Department of Functional Materials Science, Saitama University,
255 Shimo-Okubo, Sakura-ku, Saitama, Japan

A signal-to-noise ratio (S/N) is an important factor for an organic image sensor. We investigated the doping effect of silole derivative in the green-sensitive organic photoconductive device for improving S/N. The maximum S/N of 12 was achieved when 1,1-dimethyl-2,5-bis(N,N-dimethylaminophenyl)-3,4-diphenylsilole with the lowest ionization potential was used as an active layer. In addition, the graphene oxide (GO) layer was found to be an important role for decreasing the dark current density, resulting in the high S/N. The maximum S/N of approximately 20 was realized by inserting the GO layer between an indium tin oxide (ITO) anode and an active layer.

Keywords Color selectivity; green-sensitive photoconductive device; organic image sensor; organic photoconductive device; silole derivative; solution process

Introduction

Several kinds of organic thin-film devices can be fabricated by a solution process, such as inkjet printing, gravure printing, screen printing, ultrasonically spray method, and electro-spray deposition method [1–5]. Therefore, solution processed organic devices have been required for printable electronics. For example, organic light-emitting diodes, organic photovoltaic cells, and organic thin film transistors have been investigated [6–9]. Especially, several organic materials have special advantages over inorganic materials, such as the selective absorption band at a visible wavelength region, the higher absorption coefficient than inorganic semiconductors, and the possibility of the roll-to-roll printing process [10–13]. Therefore, an organic image sensor has been attracted much attention for the new development of organic devices, and it consists of stacked blue-, green-, and red-sensitive organic photoconductive devices [14,15]. This fact indicates that flexible and large-area image sensors can be realized by using organic materials instead of inorganic semiconductor materials, such as Si and GaAs.

A low-fabrication cost is another important factor for practical applications of organic image sensors, and wavelength-selective solution-processed organic photoconductive devices have been investigated [16–18]. Since a multilayer structure is difficult to be fabricated

*Address correspondence to Takeshi Fukuda, Department of Functional Materials Science, Saitama University, 255 Shimo-Okubo, Sakura-ku, Saitama 338-8570, Japan. E-mail: fukuda@fms.saitama-u.ac.jp

by a conventional solution process, the optical-to-electrical conversion efficiency of the solution processed organic photoconductive device is much lower than those of multilayer devices fabricated by the thermal evaporation process [10,17].

Our previous papers demonstrated that photoconductive characteristics of solution-processed blue-sensitive organic devices can be improved by doping silole derivative in blue-sensitive polymer, poly[(9,9-di-n-octylfluorenyl-2,7-diyl)-alt-(benzo[2,1,3]thiadiazol-4,8-diyl)] [18–21]. In addition, Seo et al. reported the green-sensitive organic photoconductive devices fabricated by the thermal evaporation process, and the highly-photoconductive characteristics, including external quantum efficiency (EQE) and S/N, have been already realized by optimizing the device structure [10].

In this paper, we investigated the solution-processed organic photoconductive device by doping silole derivative in rhodamine 6G (R6G) with the selective absorption band at the green-wavelength region [22,23]. At first, we used four kinds of silole derivatives with different ionization potentials for improving S/N [21]. Then, we also investigated an insertion effect of GO layer between an ITO anode and an active layer for decreasing the dark current density.

Experimental

A green-sensitive organic photoconductive material of R6G was dissolved in chloroform at a content of 1 wt%. Then, silole derivative was added to the resulting solution. The doping concentration of silole derivative in the R6G solution was 20 wt%. The solution was subsequently stirred at a room temperature until R6G and silole derivative were completely dissolved. We used 4 kinds of silole derivatives, such as 1,1-dimethyl-2,5-bis(*N,N*-dimethylaminophenyl)-3,4-diphenylsilole (NMe₂-silole), 1,1-dimethyl-2,3,4,5-tetraphenylsilole (H-silole), and 2,5-bis(carbazol-9'-yl)-1,1-dimethyl-3,4-diphenylsilole (PhCz-silole). The inset of Fig.1 shows molecular structures of R6G and silole derivatives.

A fabrication process of a green-sensitive organic photoconductive device is as follows. After sputtering a 150-nm-thick ITO anode on a glass substrate, the ITO-coated glass substrate was cleaned with isopropyl alcohol, acetone, and deionized water under ultrasonic waves. The sample was subsequently treated with ultraviolet ozone for 20 minutes. After spin coating the PEDOT:PSS layer at a rotation speed of 3500 rpm, the organic solution (silole derivative:R6G in chloroform) was spin coated on the ITO-coated glass substrate in a nitrogen atmosphere. And then, the sample was annealed at 70°C for 60 minutes. Finally, LiF (1 nm) and Al (150 nm) were thermally evaporated successively.

In addition, we investigated the influence of GO layer on the photoconductive characteristics of green-sensitive organic photoconductive device. The GO layer was spin coated at 2500 rpm on the ITO anode, and the measured thickness was 20 nm. The poly(9,9-di-n-octylfluorenyl-2,7-diyl) (PFO) was dissolved in chloroform at 1 wt%, and then R6G was also added in the resulting solution. The ratio of R6G:PFO was 30 wt%. Then, NMe₂-silole was also mixed, and the concentration of NMe₂-silole was changed from 10 wt% to 40 wt%. The resulting solution was spin coated on the GO layer at a rotation speed of 3500 rpm (10 wt% and 20 wt%), 4000 rpm (30 wt%), and 4500 rpm (40 wt%). Finally, LiF (1 nm)/Al (150 nm) were thermally evaporated. Fabricated devices were named as follows.

Device A: PEDOT:PSS/R6G

Device B: PEDOT:PSS/NMe₂-silole (20wt%):R6G

Device C: PEDOT:PSS/PhCz-silole (20wt%):R6G

Device D: PEDOT:PSS/H-silole (20wt%):R6G

Device E: PEDOT:PSS/NMe₂-silole (20wt%):R6G:PFO

Device F: GO/NMe₂-silole (10wt%):R6G:PFO

Device G: GO/NMe₂-silole (20wt%):R6G:PFO

Device H: GO/NMe₂-silole (30wt%):R6G:PFO

Device I: GO/NMe₂-silole (40wt%):R6G:PFO

Photocurrent and dark current-voltage characteristics were measured by using a DC voltage current source/monitor (ADCMT, 6241A). A positive bias voltage was applied to the ITO electrode by the irradiation of the green-light with the center wavelength of 525 nm. The optical intensity of excited green-light was 0.7 mW/cm². The EQE was defined as the number of output electrons divided by the total number of irradiated photons [18]. The S/N was calculated by dividing the photocurrent density by the dark current density. The absorption spectrum was recorded with a double-beam UV-Vis spectrophotometer (JASCO, V-650).

Results and Discussion

Figure 1 shows absorption spectra of used organic neat films, including R6G, NMe₂-silole, H-silole, PhCz-silole, and GO. Only the R6G neat film showed the selective absorption band at a green wavelength region. The peak absorption coefficient of R6G neat film was 31300 cm⁻¹ at 558.5 nm, and this value is high enough to absorb the incident green-light even though the thickness of active layer is several 100 nm.

On the other hand, all the silole neat films had lower absorption coefficient at a visible wavelength region than the R6G neat film. This result indicates that the green-sensitive organic photoconductive device can be realized by mixing R6G and silole derivative as an active layer.

Figure 2(a) shows the relationship between the dark current density of organic photoconductive devices with different kinds of silole derivatives and the electric field, which was calculated as the applied voltage divided by the thickness of organic layer. The measured thicknesses of organic layers were 165 nm for R6G, 200 nm for NMe₂-silole:R6G, 215 nm for H-silole:R6G, and 200 nm for PhCz-silole:R6G. In addition, the current density-electric field characteristics of device with active layer of NMe₂-silole:R6G:PFO (device E) was added in Fig. 2 to investigate the insertion effect of PFO. The current densities of all the devices with the dopant of silole derivatives were below one-tenth compared to that of the reference device with R6G only. This leads the high-S/N of the organic photoconductive device, as shown in Fig. 2(b).

Figure 2(b) shows the influence of the electric field on the S/N. The S/Ns of the devices B, C, and D were improved by doping silole derivative compared to the device A. The maximum S/N of 12 was achieved when NMe₂-silole was used as a dopant. The maximum S/N of the reference device with R6G only was 1.4; therefore, the maximum S/N of the device with NMe₂-silole was 8.5-times higher than the reference device.

Previous papers demonstrated that the photoconductive performance of blue-sensitive organic device is influenced by the ionization potential of doped silole derivative owing to the efficient carrier dislocation in the active layer [21]. In addition, the low ionization potential of silole derivative is important parameter for improving the S/N and EQE of photoconductive device [19].

In generally, several silole derivatives efficiently aggregate each other [24–26]; therefore, the low dark current density is caused by the aggregated silole derivatives in the active

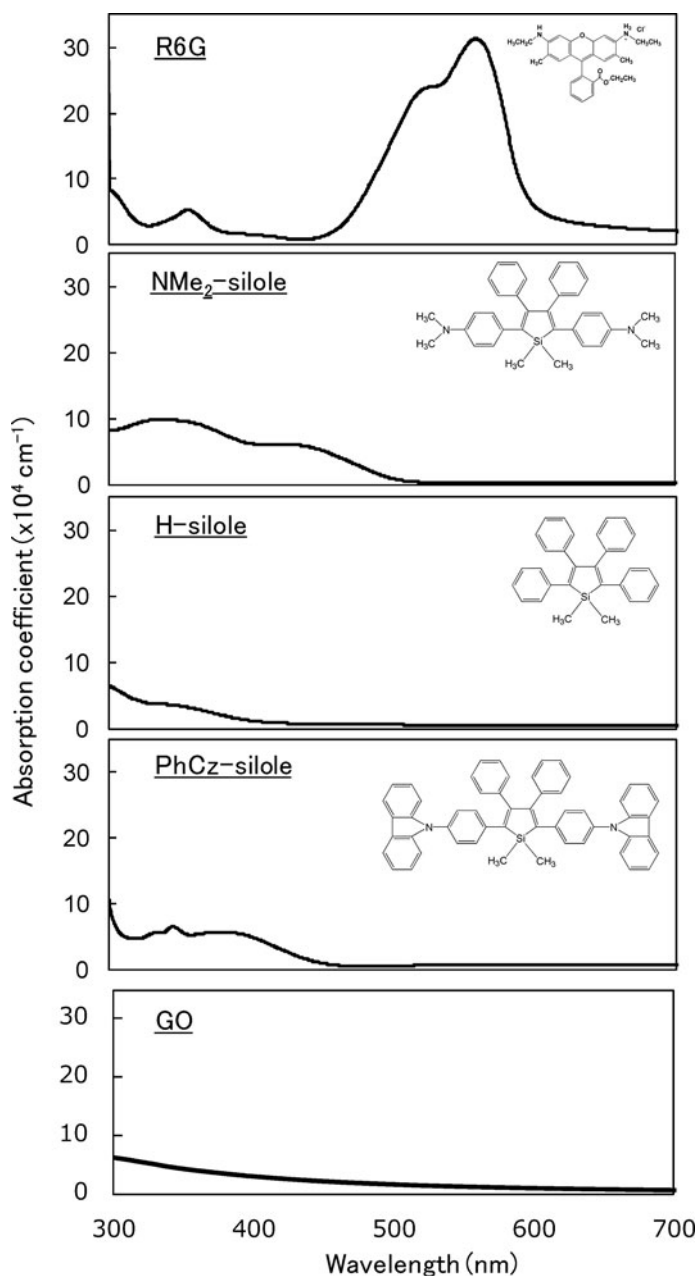


Figure 1. Absorption spectra of used organic neat films. Inset shows molecular structures of R6G, NMe₂-silole, H-silole, and PhCz-silole.

layer. In addition, the carrier dislocation efficiency can be improved by stacking, crystalline, and aggregation of organic molecule [27,28], the carrier dislocation in the active layer was considered to be occurred by the aggregation of silole derivative [21]. Therefore, the aggregated silole in the active layer caused both the efficient carrier dislocation by the irradiation of green-light and the reduced dark current density.

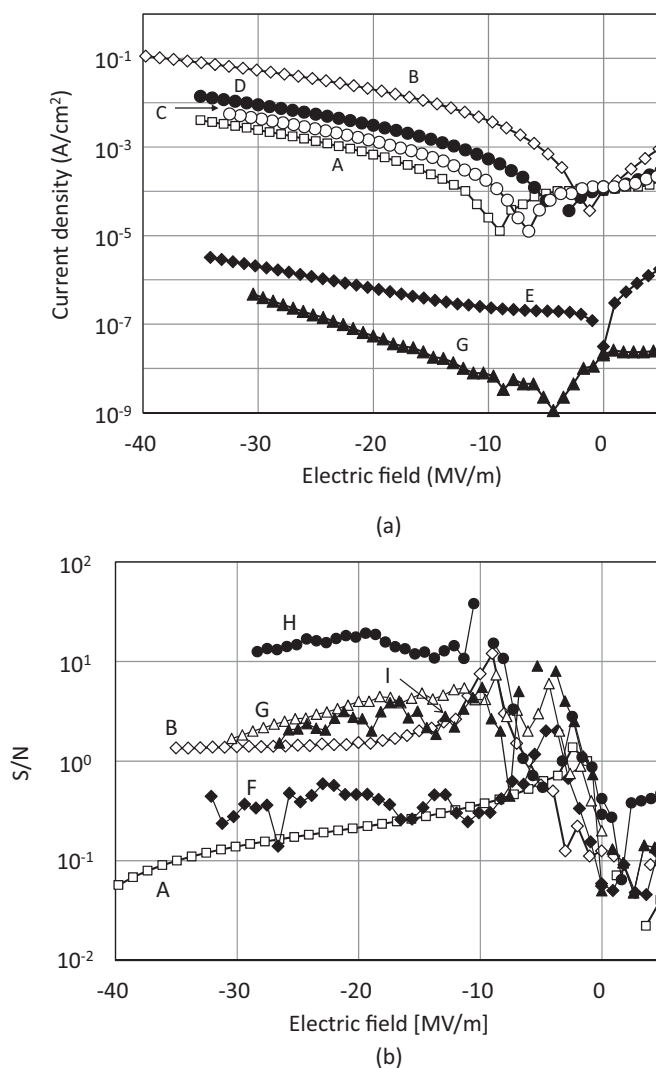


Figure 2. (a) Dark current density- and (b) S/N-electric field characteristics of organic photoconductive devices.

Furthermore, the measured ionization potentials of NMe_2 -silole, PhCz-silole, H-silole, and Naph-silole were 5.19 eV, 6.30 eV, 6.27 eV, and 5.64 eV, respectively [21]. The ionization potential of NMe_2 -silole was located between those of R6G and ITO. As a result, photo-excited carrier efficiently moves to the ITO side, resulting in the high-photocurrent density. The experimental result in Fig. 2(b) is also caused by the lower ionization potential of NMe_2 -silole than that of R6G (5.35 eV) and the aggregated NMe_2 -silole.

In addition, we will show the influence of the GO layer on the photoconductive characteristics of green-sensitive organic device. The absorption spectrum of GO neat film is shown in Fig. 1. The rotation speed of spin coat process was 3000 rpm, resulting in the thickness of 20 nm. The GO neat film has broad absorption spectrum; however, the absorption coefficient was much lower than that of R6G, as shown in Fig. 1. Therefore, the

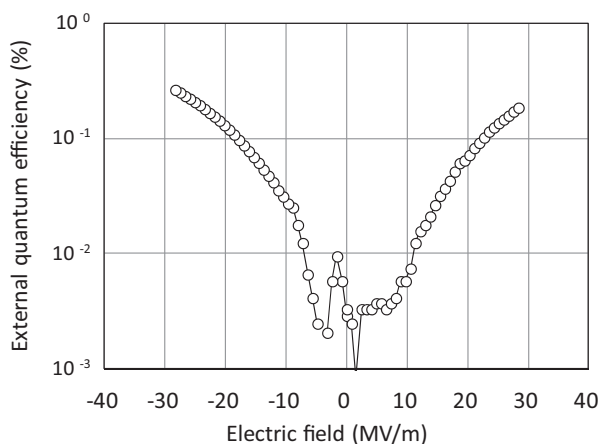


Figure 3. EQE of organic photoconductive device H with NMe₂-silole at the concentration of 30 wt%, and the GO layer was inserted between the ITO anode and the active layer.

wavelength selectivity of green-sensitive organic photoconductive device is considered to be almost same even though the GO layer is inserted between the ITO anode and the active layer.

Figure 2(b) also shows the S/N of organic photoconductive devices F-I with the GO layer, and the concentration of NMe₂-silole was changed from 10 wt% to 40wt%. The little photocurrent was observed when the thickness of GO layer was 30 nm owing to its high resistivity compared to the normal organic molecule. The S/N increased with increasing concentration of NMe₂-silole, but decreased beyond 40 wt% (device I). The most important finding is that we obtained the highest S/N was obtained at the concentration of 30 wt%. The maximum S/N was approximately 20 when the concentration of NMe₂-silole was 30 wt% (device H). This result indicates that the large amount of NMe₂-silole aggregated in the active layer. As a result, the aggregated NMe₂-silole caused the efficient carrier dislocation in the active layer [21]. However, excess aggregation prevented the carrier transport in the active layer, and the S/N decreased when the concentration of NMe₂-silole was 40 wt%. In addition, the decreased EQE at the NMe₂-silole concentration of 40 wt% was repeatable result, and the aggregation-preventing carrier transport was occurred more than the concentration of 40wt%.

Figure 3 show the EQE as a function of the electric field for the organic photoconductive device H with the NMe₂-silole at the concentration of 30 wt%, and the GO layer was inserted between the ITO anode and the active layer. The EQE linearly increased with increasing electric field, and the maximum EQE of 0.29% at -30 MV/m, corresponding to -7 V was achieved.

Conclusion

The improved S/N was realized for the green-sensitive organic photoconductive device by doping the silole derivative. In addition, the insertion of GO layer was found to be useful way for improving the S/N of organic photoconductive device.

Acknowledgment

This work was supported by JSPS KAKENHI (23750206).

References

- [1] Krebs, F. C. (2009). *Sol. Energy Mater. Sol. Cells*, 93, 394.
- [2] Steirer, K. X., Berry, J. J., Reese, M. O., van Hest, M. F.A.M., Miedaner, A., Liberatore, M. W., Collins, R. T., & Ginley, D. S. (2009). *Thin Solid Films*, 517, 2781.
- [3] Tedde, S. F., Kern, J., Sterzl, T., Früst, J., & Lugli, P. (2009). *Nano Lett.*, 9, 980.
- [4] Mo, X., Mizokuro, T., Kobayashi, A., Chen, G., Tanigaki, N., & Hiraga, T. (2008). *Thin Solid Films*, 516, 1663.
- [5] Fukuda, T., Asaki, H., Asano, T., Takagi, K., Honda, Z., Kamata, N., Ju, J., & Yamagata, Y. (2011). *Thin Solid Films*, 520, 600.
- [6] Burroughes, J. H., Bradley, D. D. C., Brown, A. R., Marks, N., Mackay, K., Fried, R. H., Burns, P. L., & Holmes, A. B. (1990). *Nature*, 347, 539.
- [7] Smilowitz, L., Sariciftci, N. S., Wu, R., Gettinger, C., Heeger, A. J., & Wudl, F. (1993). *Phys. Rev. B*, 47, 13835.
- [8] Sekitani, T., Yokota, T., Zschieschang, U., Klauk, H., Bauer, S., Takeuchi, K., Takimiya, M., Sakurai, T., & Someya, T. (2009). *Science*, 326, 5959.
- [9] Fukuda, T., Takagi, K., Asano, T., Honda, Z., Kamata, N., Shirai, H., Ju, J., Yamagata, Y., & Tajima, Y. (2012). *Jpn. J. Appl. Phys.*, 51, 02BK12.
- [10] Seo, H., Aihara, S., Watabe, T., Ohtake, H., Kubota, M., & Egami, N. (2007). *Jpn. J. Appl. Phys.*, 49, L1240.
- [11] Yang, Y., Omi, S., Goto, R., Yahiro, M., Era, M., Watanabe, H., & Oki, Y. (2011). *Org. Electron.*, 12, 405.
- [12] Higashi, Y., Kim, K.-S., Jeon, H.-G., & Ichikawa, M. (2010). *J. Appl. Phys.*, 108, 034502.
- [13] Lamprecht, B., Thüner, R., Köstler, S., Jakopic, G., Leising, G., & Krenn, J. R. (2008). *Phys. Status Sol. (RRL)*, 2, 178.
- [14] Aihara, S., Seo, H., Namba, M., Watabe, T., Ohtake, H., Kubota, M., Egami, N., Hiramatsu, T., Matsuda, T., Furuta, M., Nitta, H., & Hirao, T. (2009). *IEEE Trans. Electron. Dev.*, 56, 2570.
- [15] Seo, H., Aihara, S., Watabe, T., Ohtake, H., Sakai, T., Kubota, M., Egami, N., Hiramatsu, T., Matsuda, T., Furuta, M., & Hirao, T. (2011). *Jpn. J. Appl. Phys.*, 50, 024103.
- [16] Fukuda, T., Suzuki, T., Kobayashi, R., Honda, Z., & Kamata, N. (2009). *Thin Solid Films*, 518, 575.
- [17] Fukuda, T., Komoriya, M., Kobayashi, R., Ishimaru, Y., & Kamata, N. (2009). *Jpn. J. Appl. Phys.*, 48, 04C162.
- [18] Fukuda, T., Kobayashi, R., Kamata, N., Aihara, S., Seo, H., Hatano, K., & Terunuma, D. (2010). *Jpn. J. Appl. Phys.*, 49, 01AC05.
- [19] Kobayashi, R., Fukuda, T., Suzuki, Y., Hatano, K., Kamata, N., Aihara, S., Seo, H., & Terunuma, D. (2010). *Mol. Cryst. Liq. Cryst.*, 519, 206.
- [20] Fukuda, T., Kobayashi, R., Kamata, N., Aihara, S., Seo, H., Hatano, K., & Terunuma, D. (2010). *Jpn. J. Appl. Phys.*, 49, 01AC05.
- [21] Fukuda, T., Kimura, S., Honda, Z., Kamata, N., Mori, K., & Hatano, K. (2012). *Phys. Status Sol. (a)*, 209, 2324.
- [22] Vogel, R., Meredith, P., Harvey, M. D., & Rubinsztein-Dunlop, H. (2004). *Spectrochim. Acta A, Mol. Biomol. Spectrosc.*, 60, 245.
- [23] Dolan, G., & Goldschmidt, C. R. (1976). *Chem. Phys. Lett.*, 39, 320.
- [24] Liu, J., Lam, J. W. Y., & Tang, B. Z. (2009). *J. Inorg. Organomet. Poly. Mater.*, 19, 249.
- [25] Du, X., & Wang, Z. Y. (2011). *Chem. Commun.*, 47, 4276.
- [26] Yin, S., Peng, Q., Shuai, Z., Fang, W., Wang, Y.-H., & Luo, Y. (2006). *Phys. Rev. B*, 73, 205409.

- [27] Agostinelli, T., Lilliu, S., Labram, J. G., Campoy-Quiles, M., Hampton, M., Pires, E., Rawle, J., Bikondoa, O., Bradley, D. D. C., Anthopoulos, T. D., Nelson, J., & Macdonald, J. E. (2011). *Adv. Funct. Mater.*, 21, 1701.
- [28] Jiang, X. M., Österbacka, R., Korovyanko, O., An, C. P., Horovitz, B., Janssen, A. J., & Vardeny, Z. V. (2002). *Adv. Funct. Mater.*, 12, 587.
- [29] Pei, S., Zhao, J., Du, J., Ren, W., & Cheng, H.-M. (2010). *Carbon*, 48, 4466.
- [30] Zhu, Y., Murali, S., Cai, W., Li, X., Suk, J. W., Potts, J. R., & Ruoff, R. S. (2010). *Adv. Mater.*, 22, 3906.